A NUMERICAL ENVIRONMENT FOR PHOTOCONDUCTOR MODELING

T. Barçante Teixeira, T. de Oliveira Rocha and D. W. de Lima Monteiro

OptMA[lab] – Department of Electrical Engineering
Universidade Federal de Minas Gerais, Belo Horizonte, Minas Gerais, Brazil,
davies@ufmg.br

ABSTRACT

This work presents a model of a silicon n-type photoconductor, created within the SPICE platform, and shows the results of simulations performed on it. The model simulates the behavior of a photoconductor with respect to changes on its operating temperature, incident irradiance and changes on the doping level of the device. The resistance value of the photoconductor is also calculated by means of the insertion of the device dimensions as input data of the model.

1. INTRODUCTION

Photoconductors are, usually, two-terminal single-layered devices that find applications in very diverse fields as in automatic light activation; laser and photocopy printing; thermal-imaging arrays; display brightness control; photometry; and level indicators. A photoconductor, often termed Light-Dependent Resistor (LDR) or photoresistor, is basically a semiconductor material, with a given geometry, that produces an increase in mobile charge carriers, hence an increase in conductivity, proportional to the irradiance on it. The environment in which these devices operate is determined mostly by the spectrum and intensity of the impinging light source, operational temperature and appended circuitry. To date, there is the lack of a comprehensive numerical model capable of taking into account these factors altogether.

In order to account for the complete photoconductor modeling chain, this paper presents a numerical environment, implemented in SPICE, where we take advantage of its robust models and circuit-solving capabilities and integrate to it several aspects describing the physical environment and the photoconductor itself by means of databases, equations and semi-empirical analytical models. The approach adopted is generic and flexible in terms of spectra and photo-device. In this work, however, we chose to focus on a silicon photoconductor illuminated by the standard solar spectrum for the sake of validation.

2. PHOTOCONDUCTOR PARAMETERS

A photoconductor is usually a device made of an intrinsic semiconductor material, or with a low doping level, connected to a circuit sensitive to resistance variations. When the photoconductor is illuminated, electron-hole pairs are created in the material by means of absorption of photons. This increase in the density of carriers results in a significant reduction of the material resistivity. In the absence of light, only the thermally generated carries are available for the conduction process, the density of which is relatively small, yielding a relatively high resistivity. The resistivity of a photoconductor is calculated using equation 1.

$$\rho = \frac{1}{q[\mu_n(n+\delta n)+\mu_p(p+\delta p)]} \quad (1)$$

where q is the electron charge, n (p) is the density of electrons (holes) in darkness, δn (δp) is the density of photogenerated electrons (holes) and μ_n (μ_p) is electron (hole) mobility. The photoconductor resistance depends on the resistivity of the material and on the device dimensions, as given by equation 2.

$$R_{Photoconductor} = \rho \cdot \left(\frac{l}{d \cdot b}\right) \quad (2)$$

where ρ is the resistivity, l is the length, b is width and d is thickness of the photoconductor. Figure 1 shows a schematic drawing of a photoconductor with its dimensions.
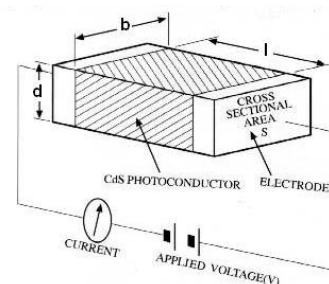

Figure 1: Schematic of a photoconductor [1]

Carrier mobilities in silicon (μ_n and μ_p), are calculated using the mathematical model MINIMOS 6 [2, 3], which takes into account changes in the carriers mobility values due to variations in temperature and due to scattering by ionized impurities in the semiconductor crystal. Additionally, MINIMOS 6 can be used to calculate the carrier mobility in Germanium, Gallium Arsenide, Aluminum Arsenide, Indium Arsenide, Indium Phosphide, and Gallium Phosphide, for n and p-type doping values.

The intrinsic carrier concentration in silicon (n_i), as a function of temperature, derives from an equation obtained from the interpolation of data from the graph shown in Figure 2.
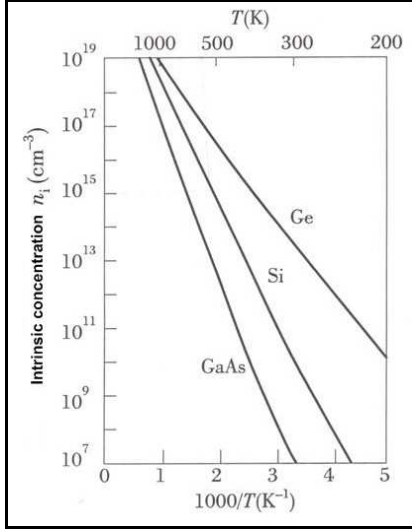

Figure 2: Intrinsic carriers concentration variation with temperature. [4]

Considering an n-type photoconductor, the value of n, in equation 1, can be equal to the donor doping level (N_d), as at room temperature, all the impurities in silicon are ionized. The hole density p is obtained by means of the law of mass action (equation 3):

$$n_i^2 = n_0 \cdot p_0 \qquad (3)$$

where the sub-index '0' represents the carrier density in darkness. When the photoconductor is illuminated by a given spectrum ($I_0 \times \lambda$), electron-hole pairs are generated by means of photon absorption. The density of photogenerated carriers is calculated with equation 4 [4].

$$\delta n = \frac{\eta_{PH} \cdot I_0 \cdot \tau_r \cdot \lambda}{h \cdot c \cdot d} \qquad (4)$$

where η_{PH} is the photoconductor quantum efficiency, I_0 is the irradiance on the photoconductor, τ_r is the carrier recombination lifetime in silicon, h is the Planck constant, c is the speed of light and d is the thickness of the photoconductor. One must observe that both, η_{PH} and I_0, are also intrinsically dependent on the wavelength λ.

The quantum efficiency η_{PH} is obtained from equation 5 [5]:

$$\eta_{PH} = \frac{J_{PH}}{q \cdot \phi_0' \cdot (1-R)} \qquad (5)$$

where J_{PH} is the photogenerated current density, R is the surface reflection coefficient and Φ'_0 is the spectral flow of photons in the photoconductor bulk. The photogenerated current density J_{PH} for the photoconductor (equation 6) is a modification of the current density at the emitter of a photodiode given by T. Markvart and L. Castañer [5].

$$J_{PH}(\lambda) = \frac{q\alpha\phi_0'(1-R)L_p}{(\alpha L_p)^2 - 1}\left[-\alpha L_p e^{-\alpha d} + \frac{S_s\frac{L_p}{D_p} + \alpha L_p - e^{\alpha d}\left(S_s\frac{L_p}{D_p}Cosh\frac{d}{L_p} + Sinh\frac{d}{L_p}\right)}{Cosh\frac{d}{L_p} + S_s\frac{L_p}{D_p}Sinh\frac{d}{L_p}}\right]$$

$$(6)$$

where α is the silicon absorption coefficient, d is the photoconductor thickness, L_p is the diffusion length of holes, D_p is the diffusion constant of holes in n-type silicon, S_s is the surface recombination velocity.

The spectral flow of photons in the photoconductor bulk is calculated in (equation 7) [5] as:

$$\phi_{PH}' = (1 - e^{-\alpha d}).10^{16}.\frac{I_0\lambda}{19.8} \qquad (7)$$

For the calculation of τ_r, an empirical formula, specific for silicon, was used (equation 8) [6].

$$\tau_r = \frac{1}{7,8 \cdot 10^{-13} \cdot N_d + 1,8 \cdot 10^{-31} \cdot N_d^2} \qquad (8)$$

3. SPICE MODELING

Using some of SPICE functions, we developed a model that simulates the behavior of silicon n-type photoconductors illuminated by a given light spectrum. This model takes as inputs the device doping level, operational temperature, incident irradiance and surface reflectivity to calculate the photoconductor resistivity. Moreover, the model allows the calculation of the device resistance, with the input of the device dimensions. To implement most of the complementary functions, we employed two features available in SPICE as voltage sources: PWL (Piecewise Linear source) and E-device. The first one provides, at its output, voltage values according to an input library (text file containing a list of values) inserted in the model. The second one is a controlled voltage source, which provides, at its output, a voltage value resulting from an embedded equation.

The photoconductor is implemented as a sub-circuit block consisting of a number of external input pins (wavelength range, irradiance, reflection coefficient and absorption coefficient) and one output terminal that provides the value of the photoconductor resistance. Internally there are several E-devices implementing equations 1 through 8, the outputs of which are voltages from the simulator perspective, but which actually correspond to pre-established traced units.

In addition to the photoconductor part, the model is composed of peripheral elements that assist in the simulation of the photoconductor. These external parts simulate: spectrum of incident light irradiation (I_0), the silicon absorption coefficient (α) and silicon reflection coefficient (R).

For the model simulation, we chose the solar spectrum AM 1.5 with a power density of 1000 W/m^2. This is the spectrum commonly used in studies involving solar irradiation. Figure 3 shows the AM 1.5 spectrum as represented inside SPICE.
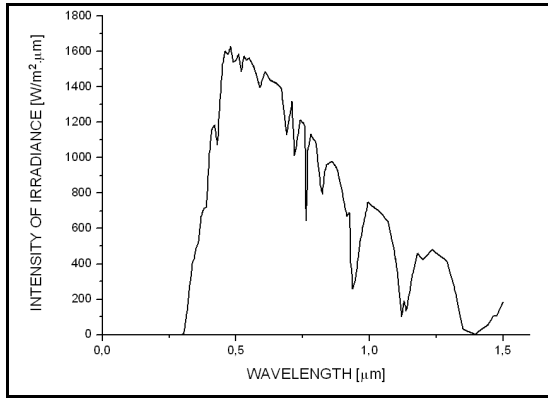
Figure 3: solar spectrum AM 1.5 represented with the model.

Figure 4 shows the silicon absorption coefficient represented at the model. It is possible to observe that for wavelengths above 1.1 μm silicon becomes transparent.
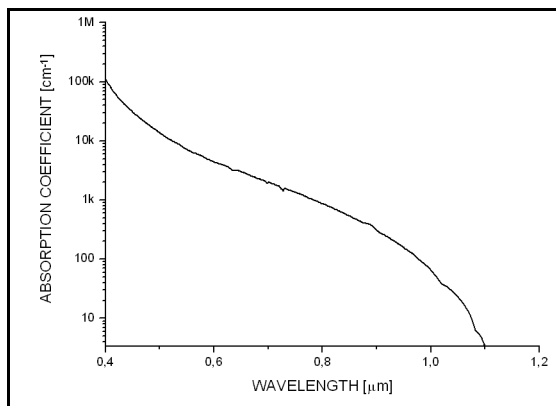

Figure 4: Silicon absorption coefficient represented with the model.

With some changes in the input parameters of the model (libraries), it is possible to simulate the absorption coefficient of other materials.

The silicon reflection coefficient depends on the wavelength of incident light. In this model, the reflection coefficient was defined as constant and equal to 10% for all values of the chosen spectrum. In practice, it is not entirely obnoxious for most of the spectrum considered, if one applies a flat broadband multi-layer anti-reflection coating.

4. RESULTS

The dark resistivity of a photoconductor varies with its doping level. The higher the doping level is, the lower will be the dark resistivity of the device, because there will be more charge carries participating in the conduction process. Figure 5 compares the model resistivity to values of a reference [7] for a device operating at 300K and in the dark.
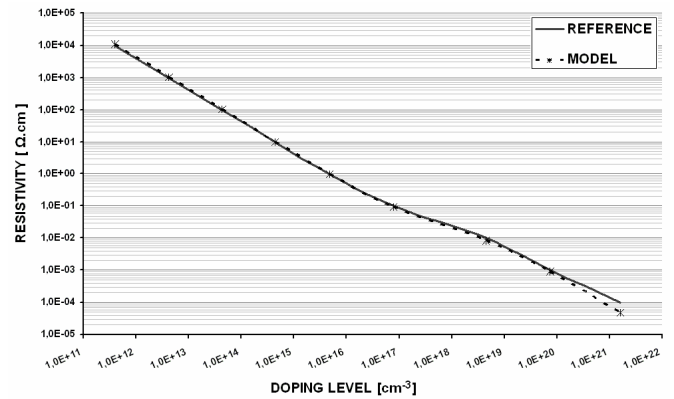

Figure 5: Variation of dark resistivity with the doping level in a n-type silicon device.

One notices that the model for the resistivity, with n-type doping, matches pretty closely that of the reference, except at very high doping levels, where degenerate effects start to play a role. This range, however, is of little practical importance to photoconductors.

The photoconductor resistance value, when it is under illumination, also varies with the semiconductor doping level. The graph of Figure 6 shows how the resistance value of an n-type silicon photoconductor, under illumination, varies with the doping level.
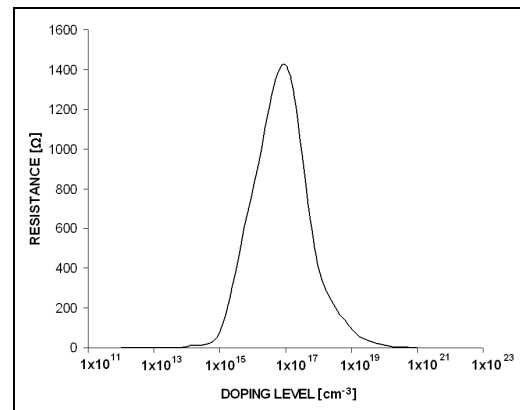

Figure 6: Variation of the photoconductor resistance under illumination with the doping level.

These values are simulation results of the photoconductor model operating at 300 K, under solar spectrum AM 1.5 and with the dimensions b x l x d (Figure 1) equal to: 0.5cm x 0.5cm x 50 μm.

Under illumination, the resistance increases with the increasing of doping level, up to the impurity level of $1x10^{17}cm^{-3}$. Above this point, the resistance value begins to decline with the increasing of the doping level. This phenomenon can be understood by the analysis of the resistivity equation (Equation 1) together with Table 1, below, which shows how the values of δn and δp vary with the doping level of the silicon photoconductor. These values result from a simulation at 300 K and under solar spectrum AM 1.5. The photogenerated electron density is considered equal to the hole density ($\delta n=\delta p$) because the electrons and holes are created in pairs.

Table 1: Variation of δn and δp with the doping level

N_d (cm^{-3})	δn = δp (cm^{-3})
1x10^{12}	8.83x10^{20}
1x10^{13}	8.83x10^{19}
1x10^{14}	8.83x10^{18}
1x10^{15}	8.83x10^{17}
1x10^{16}	8.81x10^{16}
1x10^{17}	8.63x10^{15}
1x10^{18}	7.18x10^{14}

When the doping is low, the values of δn and δp prevails over the values of n (N_d) and p in the resistivity equation (Equation 1). As the doping level increases, the values of **δn** and **δp** decrease, however, they remain dominant in the resistivity calculation (δn>>n), making the resistance values increase. From the doping level of $1x10^{17}$cm^{-3} on, the values of doping (N_d) become dominant in the equation of resistivity (n>>δn). Therefore, as doping increases, the resistance values decrease (Figure 6).

For lower doping levels, around room temperature, when the temperature increases, the mobility of electrons and holes in silicon decreases, making the photoconductor resistivity higher for each increase in temperature. Figure 7 shows the result of the simulations of the photoconductor model. The values presented are for the dark resistivity of a silicon photoconductor device with n-type doping level equal to $1x10^{15}$ cm^{-3} and illuminated by solar spectrum AM 1.5.
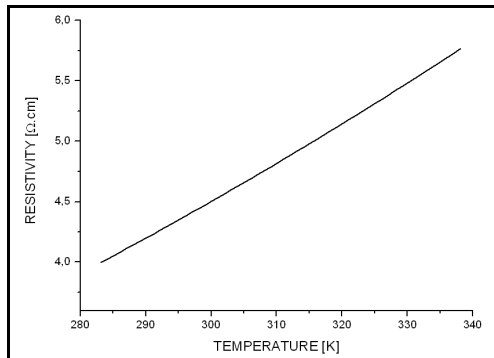

Figure 7: Photoconductor dark resistivity variation with temperature

From Figure 7, it is possible to note that the photoconductor dark resistivity value has an approximately linear variation with the temperature. Changes in photoconductor temperature cause variations in carrier intrinsic concentration (n_i) of the semiconductor (Figure 2), which causes changes in the n_o and p_o, generating changes in the resistivity value.

Table 2 shows the simulated variation of the photoconductor resistance with temperature, under illumination of the AM1.5 spectrum, $N_d=1x10^{15}$cm^{-3} and with dimensions equal to bxlxd: 0.5cm x 0.5cm x 50 μ m.

Table 2: Variation of photoconductor resistance with temperature

Temperature [K]	Resistance [Ω]
273	63,12
288	70,59
300	76,85
313	84,07
338	98,84

As the value of the dark resistance, the value of the photoconductor resistance under illumination also varies approximately linearly with temperature. Figure 8 illustrates this behavior.
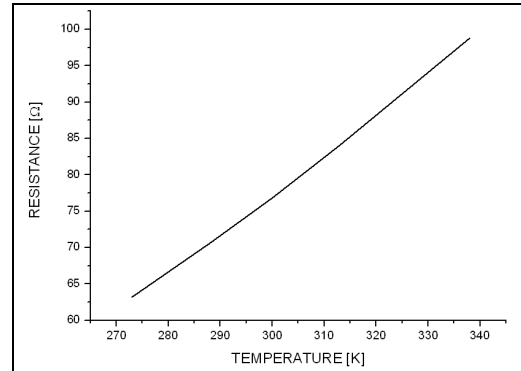

Figure 8: Variation of resistance under illumination with temperature.

5. CONCLUSIONS

The dark resistivity values, obtained from simulations performed in the n-type silicon photoconductor model, were consistent with real values. Photoconductors generally feature low doping levels, therefore, the model created can be used with accuracy, because, for doping values up to about 10^{20} cm^{-3}, the model matches the empirical resistivity results.

As expected for a silicon photoconductor with low doping, the values of resistivity under illumination with a standard solar spectrum, obtained by the model simulation, was low (in the order of mΩ). The variation of resistivity with the doping level, in the model, proved to be equally effective. This behavior can be observed in other photoconductors constructed from other semiconductor materials.

The proposed model is generic and can be used for different spectra and photo-devices by simply altering input libraries and device description blocks.

6. REFERENCES

[1] AICL - CdS Photoconductive Cells. Available at: <www.aicl.com.tw> Accessed in 10 jan. 2008.

[2] D. Caughey and R. Thomas, "Carrier Mobilities in Silicon Empirically Related to Doping and Field", *Proc.IEEE*, vol. 52, pp. 2192-2193, 1967.

[3] Mobility Model of MINIMOS 6. Available at: <http://www.iue.tuwien.ac.at/phd/palankovski/node44.html> Accessed in 10 jan. 2008.

[4] REZENDE, Sérgio M. Materiais e Dispositivos Eletrônicos. 2nd. Ed. São Paulo : Livraria da Física, 2004.

[5] T. Markvart and L. Castañer. Practical Handbook of Photovoltaics – Fundamentals and Applications. Elsevier, 2003.

[6] MOINI, Alireza. Vision Chips. 3rd Revision. Adelaide - Australia : Department of Electronics Engineering - University of Adelaide. 1997.

[7]Resistivity and Carrier Transport Parameters in Silicon. Available in: <www.virginiasemi.com/pdf/ResistivityCarrierTransportinSilicon.pdf> Accessed in 10 jan. 2008.